CrystEngComm

Accepted Manuscript

ROYAL SOCIETY OF CHEMISTRY

www.rsc.org/crystengcomm

Journal Name

RSCPublishing

COMMUNICATION

Effect of mineralization agents on surface structure and dielectric property of $SrTiO_3$ nanocrystals

Cite this: DOI: 10.1039/x0xx00000x

Lingqing Dong[a,b] , Kui Cheng[a] , Wenjian Weng[a,c,†] and Weiqiang Han[a,b,d,†]

Received 00th January 2012,
Accepted 00th January 2012

DOI: 10.1039/x0xx00000x

www.rsc.org/

In this communication, strontium titanate ($SrTiO_3$) nanocrystals with tailored surface structures have been synthesized by the hydrothermal method using sodium hydroxide (NaOH) and lithium hydroxide (KOH) as the mineralization agents. The results show that the surface structure adjusted by introducing of different mineralization agents dictate not only the corresponding size and shape but dielectric property of the obtained $SrTiO_3$ nanocrystals.

Perovskite-type metal oxide materials is of great scientific importance and technological interest for their catalytic, electric, and dielectric properties.[1,2] Strontium titanate ($SrTiO_3$), one of the most investigated perovskite materials, has large nonlinear optical coefficients, dielectric constants and chemical stability for a wide applications in fields ranging from substrate for thin-film growth[3] to electronic devices[4] and water-splitting catalysis.[5] It is well known that the surface structure, which is always strongly correlated to the growth process, is an important factor controlling the dielectric properties of perovskite materials.[6] For example, Wada et al. reported an ultrahigh dielectric constant (~15,000) of a barium titanate nanoparticle composed of a surface cubic layer and a bulk tetragonal layer.[7] They found that the dielectric constant of barium titanate nanoparticles increased with decreasing of the thickness of surface cubic layer, which could be controlled by the degree of vacuum during preparation process.

Furthermore, we appreciate that surface structure of nanocrystals not only determine their properties but also the process of crystal growth (resultant morphology), which is actually a surface or interface reaction. Therefore, it is desirable to shed light on the relationships between the surface structure of $SrTiO_3$ nanocrystals and crystal growth process as well as their dielectric properties.

We have recently reported the synthesis of $SrTiO_3$ nanocrystals with perfect cubic morphology by using LiOH as the mineralization agent.[8] However, these previous efforts have only reported the final morphology of nanocrystals. The observations still show a lack of the effects of LiOH on $SrTiO_3$ nanocrystals morphology that compared with other commonly-used mineralization agent, such as KOH, during the growth process. Moreover, significant scope of the differences in properties by using these two different mineralization agents still needs to be explored. In this work, we study the effects of mineralization agent (LiOH compared to KOH) on the surface structure and morphology of $SrTiO_3$ nanocrystals. And their dielectric properties including dielectric constant and loss are also investigated.

In a typical synthesis, 0.265 ml of $TiCl_4$ (Aladdin, 99%) was dropwised into 25ml of deionized water cooled in an ice bath. After stirring for 5 min, 30 ml of 3M LiOH (Aladdin, 98%) or KOH (Aladdin, 95%)solution and 10 ml of 0.24M $SrCl_2$ (Aladdin, 99.5%) solution were orderly added. The resultant solution was then sealed in a Teflon-lined stainless steel autoclave and maintained at 180 °C for 6 h. After the reaction, the resulting precipitate was centrifugally separated and washed with ethanol and water. The morphology and microstructure of obtained $SrTiO_3$ nanocrystals were measured by a field-emission scanning electron microscopy (FESEM, HITACHI SU70) and a transmission electron microscopy (TEM, FEI JEM-2100). The crystal structure of the specimens was studied by X-ray power diffraction microdiffractometer (XRD, PANalytical X'Pert Pro, Netherlands). The dielectric properties including dielectric constant and loss were measurted using an impedance analyzer (Agilent 4294 A) in a wide frequency (40~150M Hz) at ambient temperature.

Fig. 1a and b show a typical representative scanning electron microscopy (SEM) and transmission electron microscopy (TEM) images of the $SrTiO_3$ nanocrystals synthesized by using KOH as the mineralization agent, respectively. The average nanoparticle size of $SrTiO_3$ nanocrystals is estimated to be about 200 nm, based on the observation of SEM and TEM images. Furthermore, it can be seen that the surface of nanocrystals appear to be smooth and the morphology of $SrTiO_3$ nanocrystals are cube with rounded edges (edge-truncated cube), which can be apparently observed in Fig. 1c. To examine the surface structure of $SrTiO_3$ nanocrystals, high-resolution transmission electron microscopy (HRTEM) analysis is performed on the edge of one $SrTiO_3$ nanocrystal. As indicated in Fig. 1d, a core-shell surface structure is clearly observed. The thickness of the shell layer is in the range 3~5 nm. Further energy

dispersive X-ray spectroscopy (EDS) analysis of the core-shell surface structure reveal a Sr-deficient composition, as shown in Fig. 1e and f.

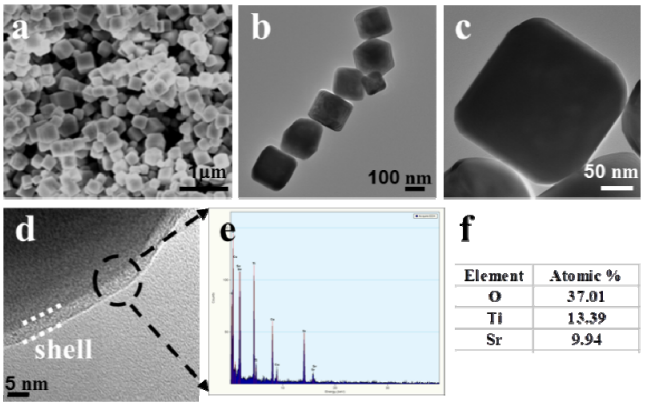

Fig. 1 SEM image (a) and TEM image (b) of $SrTiO_3$ nanocrystals synthesized by using KOH as the mineralization agent, (c) a cube with rounded edges of single $SrTiO_3$ nanocrystal and a core-shell surface structure is observed in (d), (e) EDS analysis of the core-shell surface (a portion marked with a circle in ''d'') and the quantitative analysis of O, Ti and Sr elements (f).

To gain insight into the effects of different mineralization agent on the morphology and surface structure of $SrTiO_3$ nanocrystals in this system, we carry out a comparative experiment by using LiOH as the mineralization agent. In this case, the obtained $SrTiO_3$ nanocrystals are perfect cubic morphology with sharp right angle corners, as shown in Fig. 2a and b. The average nanoparticle size of $SrTiO_3$ nanocrystals is also estimated to be about 200 nm, the same as the products obtained by using KOH as the mineralization agent. However, there is no core-shell surface structure observed in HRTEM image of a typical $SrTiO_3$ nanocrystal edge (Fig. 2c). Meanwhile, a few small nanoparticles with ~5 nm size are observed to adsorb on the surface of $SrTiO_3$ nanocrystal, as indicated in Fig. 2d. To determine the composition of the small nanoparticles, EDS analysis is also carried out. The results indicate that there is very few Sr element containing in the adsorbed small nanoparticles, as shown in Fig. 2e and f.

Usually, NaOH or KOH are used as the mineralization agent to prepare the perovskite materials.[9-15] The obtained products are often observed a surface core-shell structure, which is regarded as defects such as OH^- defects and cationic vacancies. For example, Zhu et. al observed a core-shell surface structure of $BaTiO_3$ nanocrystals with 2~3.5 nm thickness shell layer by using a hydrothermal method with KOH as the mineralization agent.[6] These results are consistent with our experimental observation, as shown in Fig. 1d. Normally, the OH^- defects can be produced easily once the dehydration process of $TiO_2{\cdot}nH_2O$ gel during the crystal growth is not complete.[16, 17] Therefore, the OH^- defects are the main form of the defect in hydrothermal/solvothermal growth of perovskite nanocrystals in high-alkaline solution. On the other hand, Li^+ is considered to facilitate the dehydration of surface OH^- adsorbed on crystal surface and disturb the composition and structure of liquid layer on interface, reducing the resistance of adsorbed layer on crystal growth and the probability of OH^- ions diffusing into the crystal lattice. Therefore, when LiOH is introduced as the mineralization agent, there is no core-shell surface structure observed in $SrTiO_3$ nanocrystals edge, and the morphology of obtained $SrTiO_3$ nanocrystal appear to be perfect cubic morphology with sharp right angle corners. However, there are a few small nanoparticles adsorbed on surface of $SrTiO_3$ nanocrystals, as HETEM results shown in Fig. 2d. These small nanoparticles are amorphous (data not shown), and the composition is almost consistent with $TiO_2{\cdot}nH_2O$ gel (Fig. 2e and f). They can be regarded to be took off from the "shell" due to the dehydration effects of Li^+ and can be eliminated easily by Ostwald ripening process when the duration increase, as shown in our recently reported work.[8] Furthermore, the Li^+ can be removed by washing process, as the X-ray photoelectron spectrum (XPS) results shown (data not shown). These results indicate that the surface structure of nanocrystals during the growth process plays an important role in determining the final morphology of obtained products.

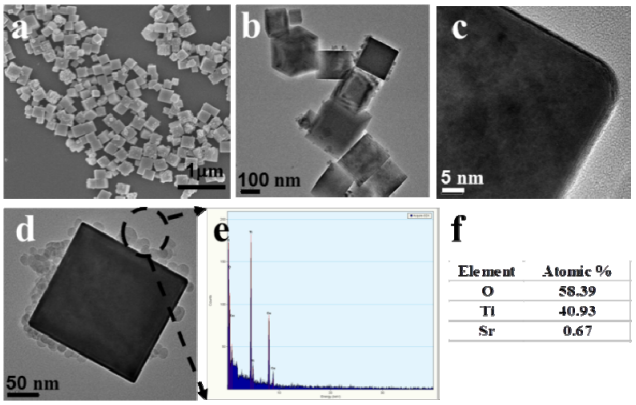

Fig. 2 SEM image (a) and TEM image (b) of $SrTiO_3$ nanocrystals synthesized by using LiOH as the mineralization agent, (c) there is no core-shell surface structure observed in a single $SrTiO_3$ nanocrystals edge, (d) a perfect cube $SrTiO_3$ nanocrystal with a few small nanoparticles (~5 nm) adsorbed on its surface, (e) EDS analysis of the small nanoparticles (a portion marked with a circle in ''d'') and the quantitative analysis of O, Ti and Sr elements (f).

X-ray diffraction (XRD) patterns of the $SrTiO_3$ nanocrystals synthesized by using KOH and LiOH as the mineralization agents are shown in Fig. 3, in which all the diffraction patterns match well with those of cubic $SrTiO_3$ phase (JCPDS No. 35-0734). And these results are consistent with the experimental results of V. Buscaglia et al.. Furthermore, it is noteworthy that the ratio of the intensity of the (220) peak to that of the (200) peak is 0.30 for the perfect cubes and 0.37 for the edge-truncated cubes, respectively, an increased trend that can be rationally related to the increasing of the fractions of {110} facets.[18] These results appear to further confirm the SEM and TEM observation.

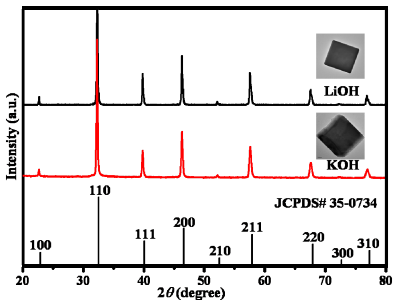

Fig. 3 XRD patterns of the $SrTiO_3$ nanocrystal products synthesized by using KOH and LiOH as the mineralization agents. Pattern (vertical lines) of JCPDS 35-0734 ($SrTiO_3$) is also provided.

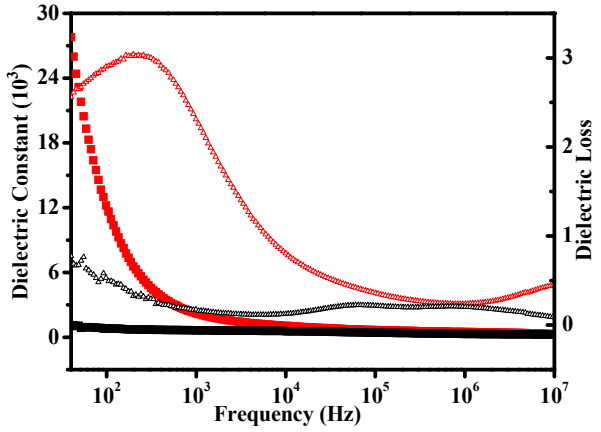

Fig. 4 Dielectric properties of the $SrTiO_3$ nanocrystal products synthesized by using KOH (red curves) and LiOH (black curves) as the mineralization agents. Curves with solid square and hollow triangle are dielectric constant and loss, respectively.

The dielectric properties of perovskite materials are considered to be sensitive to their surface structures, especially surface defects of nanocrystals.[19-21] To study the effects of surface structure of $SrTiO_3$ nanocrystals on their dielectric properties, we investigate the dielectric constant and loss of the two typical $SrTiO_3$ nanocrystals, as shown in Fig. 4. The obtained $SrTiO_3$ nanocrystals synthesized using LiOH as the mineralization agent show exceptionally low values of dielectric constant and loss upon the frequency increasing from 40 to 150M Hz. These are because in its pure, unstressed and defect-free form, $SrTiO_3$ is paraelectric.[22] On the other hand, the obtained $SrTiO_3$ nanocrystals synthesized using KOH as the mineralization agent show a very high value of dielectric constant (>10k) at low frequencies (<10k Hz), and decreases continuously to a stable value the same as the other $SrTiO_3$ nanocrystals (synthesized using KOH as mineralization agent) at frequency of 10^4 Hz. The dominant mechanisms for dielectric properties at low frequencies are considered to dipolar polarisation and polarisation due to the separation of free charges in the sample, which can be attributed to the adsorbed dipoles on surface and the existence of permanent dipoles in material. Therefore, the anomalous dielectric behavior of the $SrTiO_3$ nanocrystals synthesized using KOH as the mineralization agent might be assigned to their surface core-shell structure with OH^- defects, as reported previously.[23] It also shows a relative high dielectric loss at low frequencies (<10k Hz), which might be attributed to the space charge polarization correlated to the surface defects of $SrTiO_3$ nanocrystals.[24]

Conclusions

In summary, $SrTiO_3$ nanocrystals with tailored surface structures have been synthesized by using KOH and LiOH as the mineralization agents. Perfect cubic morphology with sharp right angle corners of $SrTiO_3$ nanocrystals are obtained by using LiOH as the mineralization agents thanks to the dehydration effects of Li^+. The surface core-shell structure, OH^- defects due to the incomplete dehydration process of $TiO_2 \cdot nH_2O$ gel during the crystal growth, has been observed in $SrTiO_3$ nanocrystals obtained using KOH as the mineralization agent. These special surface structures give rise to the anomalous dielectric behavior of the $SrTiO_3$ nanocrystals. Based on the ultraviolet-visible (UV-Vis) diffuse reflectance spectra (data not shown), the band gap energy (Eg) of $SrTiO_3$ nanocrystals synthesized by using LiOH and KOH as the mineralization agents are 3.58 eV and 3.56 eV, respectively, which are consistent with the calculational results.[25] The giant dielectric constant of $SrTiO_3$ nanocrystals with surface defect structures in this work show a potential application of paraelectric ceramics as passive components in capacitors instead of ferroelectric due to no phase transition. Moreover, the crystal growth process can dictate that of the corresponding surface structure of nanocrystals and their properties, an idea which has implications for nanoscale design as well as for exploring of surface structure-dependent properties in nanomaterials.

Acknowledgements

This work was supported by the National Basic Research Program of China (973 project, 2012CB933600), the National Natural Science Foundation of China (Grant No. 51072178, 51272228 and 81071258). W.H. thanks the support from the Project of the Ningbo 3315 International Team.

Notes and references

[a] Department of Materials Science and Engineering, State Key Laboratory of Silicon Materials, Cyrus Tang Center for Sensor Materials and Applications, Zhejiang University, Hangzhou 310027, China
[b] Ningbo Institute of Materials Technology & Engineering, Chinese Academy of Sciences, Ningbo 315210, China
[c] Shanghai Institute of Ceramics, Chinese Academy of Sciences, Shanghai 200050, China
[d] School of Physical Science and Technology, ShanghaiTech University
† Correspondence and requests for materials should be addressed to: wengwj@zju.edu.cn and hanweiqiang@nimte.ac.cn

1. M. A. Pena and J. L. G. Fierro, *Chem. Rev.*, 2001, **101**, 1981-2017.
2. B. Parija, S.K. Rout, L.S. Cavalcante, A.Z. Simões, S. Panigrahi, E. Longo and N.C. Batista, *Appl. Phys. A* 2012, **109**, 715–723.
3. A. Ohtomo and H. Y. Hwang, *Nature*, 2004, **427**, 423-426.
4. C. Cen, S. Thiel, J. Mannhart and J. Levy, *Science*, 2009, **323**, 1026-1030.
5. T. K. Townsend, N. D. Browning and F. E. Osterloh, *Acs Nano*, 2012, **6**, 7420-7426.
6. X. H. Zhu, Z. G. Zhang, J. M. Zhu, S. H. Zhou and Z. G. Liu, *J. Cryst. Growth*, 2009, **311**, 2437-2442.
7. S. Wada, T. Hoshina, K. Takizawa, M. Ohishi, H. Yasuno, H. Kakemoto, T. Tsurumi, C. Moriyoshi and Y. Kuroiwa, *J. Korean Phy. Soc.*, 2007, **51**, 878-881.
8. L. Q. Dong, H. Shi, K. Cheng, Q. Wang, W. J. Weng and W. Q. Han, *Nano Res.*, 2014, **ASAP**.
9. L. F. Silva, W. Avansi, J. Andres, C. Ribeiro, M. L. Moreira, E. Longob and V. R. Mastelaro, *Phys.Chem. Chem. Phys.*, 2013, **15**, 12386-12393.
10. V. R. Calderone, A. Testino, M. T. Buscaglia, M. Bassoli, C. Bottino, M. Viviani, V. Buscaglia and P. Nanni, *Chem. Mater.*, 2006, **18**, 1627-1633.

11. Y. Cao, K. J. Zhu, J. S. Liu and J. H. Qiu, *Adv. Powder Tech.*, 2014, **25**, 853-858.
12. N. H. Park, Y. F. Wang, W. S. Seo, F. Dang, C. C. Wan and K. Koumoto, *CrystEngComm*, 2013, **15**, 679–685.
13. S. Adireddy, C. K. Lin, B. B. Cao, W. L. Zhou and G. Caruntu, *Chem. Mater.* 2010, **22**, 1946–1948.
14. W. J. Dong, X. Y. Li, J. Yu, W. C. Guo, B. J. Li, L. Tan, C. R. Li, J. J. Shi and G. Wang, *Mater. Lett.* 2012, **67**, 131-134.
15. G. Xu, S. Q. Deng, Y. F. Zhang, X. Wei, X. Yang, Y. Liu, G. Shen and G. R. Han, *CrystEngComm*, 2014, **16**, 2025–2031.
16. J. X. Lei, X. L. Liu and J. F. Chen, in *Aicam 2005*, eds. M. Nogami, R. Jin, T. Kasuga and W. Yang, 2006, vol. 11-12, pp. 23-26.
17. S. C. Zhang, J. X. Liu, Y. X. Han, B. C. Chen and X. G. Li, *Mater. Sci. Eng. B-Adv.*, 2004, **110**, 11-17.
18. W. C. Huang, L. M. Lyu, Y. C. Yang and M. H. Huang, *J. Am. Chem. Soc.*, 2012, **134**, 1261-1267.
19. Q. Yu, D. Liu, R. J. Wang, Z. B. Feng, Z. Y. Zuo, S. B. Qin, H. Liu and X. G. Xu, *Mater. Sci. Eng. B-Adv.*, 2012, **177**, 639-644.
20. Y. He, H. W. Zhang, P. Liu, J. P. Zhou and C. H. Mu, *Physica B*, 2009, **404**, 3722-3726.
21. S. K. Thatikonda, D. Goswami and P. Dobbidi, *Ceram. Int.*, 2014, **40**, 1125-1131.
22. J. H. Haeni, P. Irvin, W. Chang, R. Uecker, P. Reiche, Y. L. Li, S. Choudhury, W. Tian, M. E. Hawley, B. Craigo, A. K. Tagantsev, X. Q. Pan, S. K. Streiffer, L. Q. Chen, S. W. Kirchoefer, J. Levy and D. G. Schlom, *Nature*, 2004, **430**, 758-761.
23. D. Singh, P. Yadav, N. Singh, C. Kant, M. Kumar, S. D. Sharma and K. K. Saini, *J.Exp. Nanosci.*, 2013, **8**, 171-183.
24. W. W. Cho, I. Kagomiya, K. I. Kakimoto and O. Hitoshi, *J. Eur. Ceram. Soc.*, 2007, **27**, 2907-2910.
25. S. Piskunov, E. Heifets, R.I. Eglitis, G. Borstel, *Comput. Mater. Sci.,* 2004, **29**, 165-178.